The Physics of Chromospheric Plasmas
ASP Conference Series, Vol. 368, 2007
Petr Heinzel, Ivan Dorotovič and Robert J. Rutten, eds.

Solar Cycle Variation of Chromospheric Radiation

S. K. Solanki

MPI für Sonnensystemforschung, Katlenburg-Lindau, Germany

Abstract. Radiation emitted by the Sun's chromospheric gas displays a significant cyclic variation. The magnitude of this variability and the shape of the light curve differs from that exhibited by photospheric radiation, or total solar irradiance. The amplitude of the cyclic variation of chromospheric radiation is larger and less affected by the contribution of sunspots. Consequently, the influence of small-scale magnetic features forming plage and the network dominates. Here a brief introduction is given to the solar cycle variation of chromospheric radiation, its connection with the magnetic field, its quantitative modeling and related questions, such as the solar cycle variability of the quiet Sun chromosphere and its cause. Finally, some thoughts on the possible secular change of chromospheric (and total) irradiance are presented.

1. Introduction

Most solar phenomena are found to vary over the solar cycle. As the cycle progresses the number of features such as sunspots, faculae, plage, coronal loops or active regions change, as does the solar surface area covered by such features. In addition, global solar properties, such as the total or spectral solar irradiance, also evolve in phase with the solar activity level. Irradiance is the solar radiative flux measured above the Earth's atmosphere (normalized to a mean distance of 1AU from the Sun). The irradiance in a restricted wavelength range is called the spectral irradiance, while integrated over the whole spectrum it is termed the total irradiance.

Along with the radiation from other layers of the atmosphere, the radiation from the chromosphere varies over the activity cycle. The cause of this variation, at all scales, is thought to be localized in individual concentrations of the Sun's magnetic field: As the number of facular elements (magnetic elements) increases, so does their combined output at chromospheric wavelengths. Together, these local contributions add up to a change in the global chromospheric radiative output, i.e. chromospheric irradiance.

In this paper I provide an overview of the change in the chromospheric radiation (both local and global) and how it is related to the underlying magnetic field.

2. Solar Irradiance Variations: Different Atmospheric Layers

Figure 1 shows the variation of solar irradiance in different wavelength bands reflecting different layers of the solar atmosphere. The total solar irradiance

(TSI), the Mg II core-to-wing index and the F10.7 cm flux are plotted along with two activity indicators, the sunspot number, R_Z, and sunspot area, A_S.

Although the TSI gets contributions from all emitting layers of the solar atmosphere, the lion's share comes from the photosphere (> 95%, Solanki & Unruh 1998). Hence the TSI indicates variations of the photospheric contribution to irradiance (although these variations are dominated by the contributions of the spectral lines, Mitchell & Livingston 1991; Unruh et al. 1999). Plotted is the PMOD composite due to Fröhlich (2005), which has been put together from measurements recorded by instruments flying on different satellites. TSI composites that deviate to a lesser or larger degree from the plotted one have been published by Willson & Mordvinov (2003) and DeWitte et al. (2004). They differ partly in the data sets used and in particular in the applied corrections for degradation of instrumental sensitivity etc.

The relative amplitude of the TSI variation over the solar cycle is only 0.1% and there is a qualitative difference between the daily (dotted) and monthly running mean values (solid). The daily values show individual strong downward excursions lasting typically around a week, while the excursions in the positive direction are significantly weaker. The monthly averages are much more symmetric as far as short-term variations are concerned. These fluctuations are restricted mainly to the periods around the maximum of the activity cycle. The downward excursions are due to the passage of sunspots over the solar disk (they do not last quite 2 full weeks because of foreshortening effects and because the faculae surrounding sunspots are increasingly bright near the limb where they increasingly compensate the sunspot darkening. The upward excursions are due to faculae. They appear when active regions are close to the solar limb, where the faculae actually dominate over the spots, but are partly due to older, decaying active regions whose sunspots have decayed so that the active regions are composed entirely of faculae.

The Mg II core-to-wing ratio or Mg-index is, as the name suggests, the ratio of the irradiance in the cores of the Mg II h and k lines relative to the irradiance in their wings (Heath & Schlesinger, 1986; Deland & Cebula 1998; Viereck & Puga 1999; Viereck et al. 2001). Taking the ratio between the irradiance at two wavelengths that lie relatively close to each other has the advantage that, the instrumental degradation at both wavelengths being roughly the same, this quantity is nearly independent of instrumental degradation. Since the variation in the chromospheric Mg II h and k line core is much larger than in the wings of these lines (formed in the photosphere), this index mainly represents the chromospheric excess radiation relative to the photosphere. Note the much larger relative variation (roughly 6–7%) compared to the TSI and the fact that the daily points are relatively symmetrically distributed around the monthly curve. Not surprisingly, the correlation coefficient between the daily Mg II index and the TSI is rather low, with a correlation coefficient of $r_c = 0.52$. However, the monthly running means correlate rather well ($r_c = 0.80$). The difference in behaviour to the TSI light curve is mainly because the sunspots do not contribute significantly to the Mg index.

The 10.7 cm radio flux (Tapping, 1987; Tapping & Detracey 1990) has a coronal source. Here the flux (irradiance) varied by a factor of roughly 2.5 over the last three cycles. Although the general shape of the cyclic changes is similar to that shown by the Mg II index, the short term fluctuations (around cycle

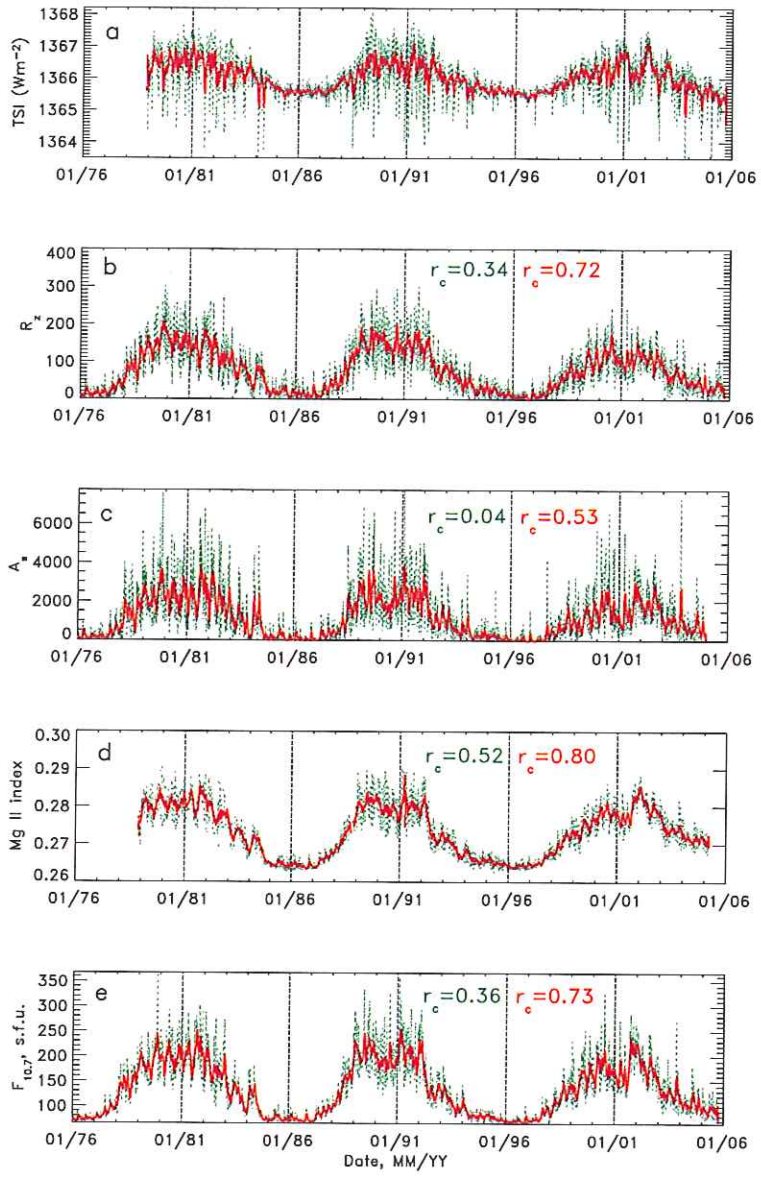

Figure 1. a) Total solar irradiance (TSI) vs. time. The dotted (green in the electronic version) line represents daily measurements, the solid (red) line, monthly averages. b) Sunspot number, R_Z. Correlation coefficients between the plotted curves and the total irradiance are given (the number on the left refers to daily values, the one on the right to monthly means). c) Sunspot area, A_S, i.e. the area covered by all sunspots in ppm of the solar disk. d) Mg II k core-to-wing ratio (Mg II index). e) F10.7, i.e. flux at 10.7 cm. Figure kindly provided by N. A. Krivova.

maxima) are considerably larger. Consequently the correlations of both the daily and the monthly smoothed time series with the corresponding TSI time series are lower ($r_c = 0.36$ and 0.73, respectively) than for the Mg index.

3. Irradiance and Magnetic Field

There is strong evidence that the changes in the irradiance arising from all atmospheric layers are due to the evolution of magnetic features on the solar surface. Magnetic features can lead to either a local brightening roughly cospatial with the magnetic field (bright points forming faculae in the photosphere, plage in the chromosphere and the network), or a local darkening at the solar surface (pores, sunspots). Quite instructive is to consider the dependence of the brightness emanating from different layers on the magnetogram signal (longitudinal magnetic field strength averaged over the spatial resolution element). Already the early work by Frazier (1971), illustrated in Fig. 2, showed just how different this dependence is for the photosphere and the chromosphere. The upper frame (b) shows the Ca II K core contrast (the relative difference between the intensity at a given magnetogram level and the quiet Sun intensity, i.e. the intensity at null magnetogram signal) plotted vs. magnetogram signal, while in the lower frame (a) the contrast of the continuum intensity in the green part of the solar spectrum is plotted. The dots are individual positions on the solar disk, while the solid lines are trend curves. Both sets of measurements refer to the center of the solar disc.

Clearly, whereas in the photosphere the contrast initially increases slightly with magnetogram signal, reaching a maximum contrast of roughly 0.035 at around 200 G and then decreases again to the extent that above 500 G it becomes negative (i.e. the magnetic features are darker than the quiet photosphere). This is not unexpected, since the largest magnetogram signals are shown by pores and sunspot umbrae, both of which are dark. Indeed it has recently been shown that sunspot umbrae are darker for increasing area of the magnetic structure (see Mathew et al. 2007). This basic behaviour is also revealed by newer studies (e.g., Topka et al. 1997; Ortiz et al. 2002), although closer to the solar limb the turnover point where the contrast starts decreasing again moves to increasingly higher magnetogram signals. Thus, small pores are dark at disk cemtre, but can appear bright near the limb.

The contrast of the chromospheric radiation, however, shows no sign of decreasing again for large magnetogram signals, although the rise slows (cf. Schrijver et al. 1989; Solanki et al. 1991). Schrijver et al. found that they could describe the dependence on the field of the Ca II K core contrast by a power law of the form $\langle B \cos\theta \rangle^{0.6}$. Cores of photospheric spectral lines lie in between the two extreme behaviours illustrated above.

4. Influence of Magnetic Features on Brightness

The dependence of the brightness or contrast on magnetic flux in the resolution element can be at least qualitatively understood by considering the sketch shown in Fig. 3, which has been adapted from a figure in Zwaan (1978). It shows a schematic magnetic flux tube (the boundaries or side walls of the flux tube are

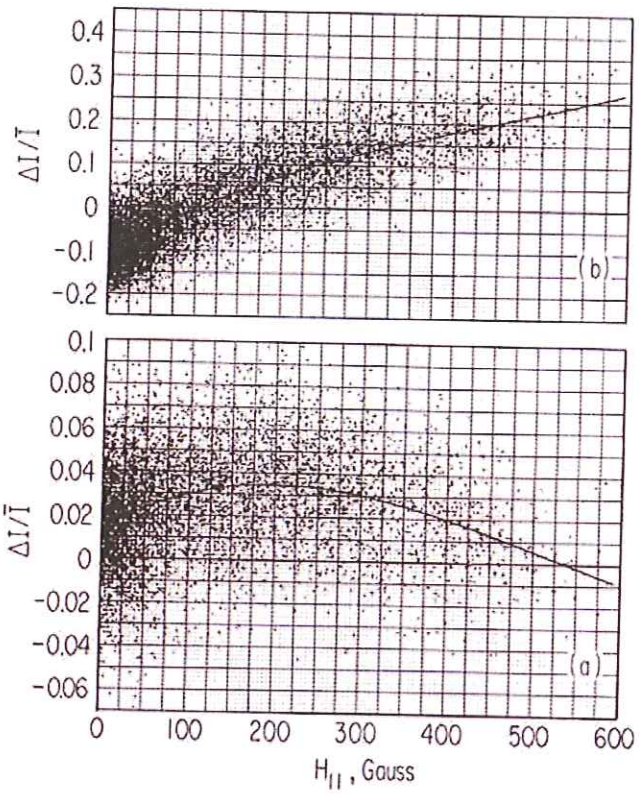

Figure 2. Intensity contrast, $\Delta I/\langle I\rangle = (I(H_{||}) - I(H_{||} = 0))/\langle I(H_{||}\rangle$, vs. magnetogram signal $H_{||}$. Upper panel (b): Ca II K line core. Lower panel (a): continuum in the green part of the solar spectrum. Figure adapted from Frazier (1971).

represented by the curved, nearly vertical lines) passing through the solar surface (indicated by the thick horizontal lines, with the solar surface lying at a lower level in the flux tube due to its evacuation). In the subphotosphere the magnetic field leads to a reduction in the efficiency of convection (heat blocking), indicated in Fig. 3 by the vertical (red) arrows (internal vertical energy flux $F_i \ll F_e$). This is compensated by the lateral inflow of radiation into the flux tube (F_r) through the walls at a level lying above the internal $\tau = 1$ surface and the external $\tau = 1$ surface, indicated by the upper horizontal (yellow) arrows. For a strong field that almost completely blocks the internal convective transport, to first order the amount of heating depends on the ratio of the wall area to the area of the flux tube's cross section (although other factors, such as the properties of the surrounding gas also play a role; cf. Deinzer et al. 1984a,b; Vögler et al. 2005). If the flux tube is small, then the inflowing radiation can more than compensate the blocked vertical energy flux, leading to a positive contrast of the magnetic features. This simple model also, at least qualitatively, explains the centre-to-limb behaviour of the contrast, in particular the brightening seen

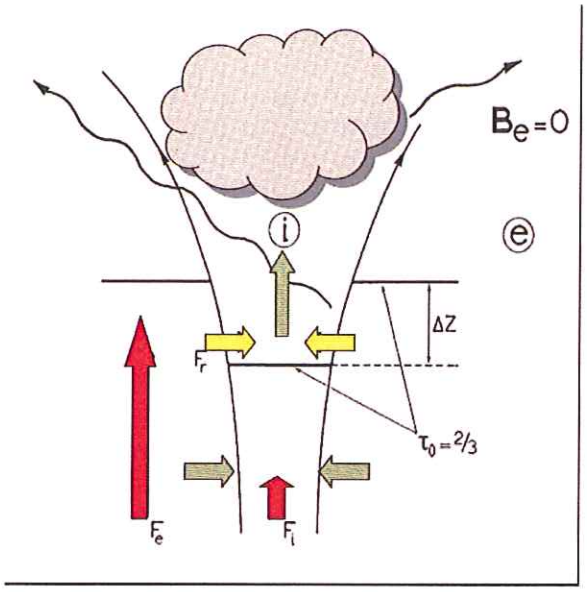

Figure 3. Sketch of a magnetic flux tube and the processes leading to excess radiation emerging from it in the photosphere and the chromosphere. See text for details. Adapted from Zwaan (1978).

away from disk centre, as the hot walls become visible (indicated in Fig. 3 by the long wavy arrow leaving the right wall towards the upper left).

For the chromospheric radiation the underlying physics is expected to be significantly different, and has been worked out in less detail than the simpler photospheric case. The classical picture is that in addition to radiation, mechanical energy is laterally introduced into the magnetic feature by the turbulent medium in which it is embedded. This buffetting by the neighbouring convection cells is clearly seen in the 2-D numerical simulations of Steiner et al. (1996), although it is likely that the effect is exaggerated somewhat in 2-D, since the granular flows cannot work their way round the flux tube, which is the case in 3-D. Convection excites different MHD wave modes that travel up along the field (e.g., Huang et al. 1995). These can be longitudinal, tube waves (e.g., Roberts & Webb 1978; Musielak et al. 2000), transverse modes (Musielak and Ulmschneider 2002) or torsional Alfvén waves (Noble et al. 2003). See e.g., Narain and Ulmschneider (1996); Roberts and Ulmschneider (1997), Carlsson & Hansteen (2005) for overviews. The energy input by the granular buffeting is indicated in Fig. 3 by the lower pair of horizontal (green) arrows.

These waves carry a given energy flux into the chromosphere, indicated by the upper vertical (green) arrow. In the case of the magneto-acoustic tube mode the energy can be dissipated in the chromospheric layers through the formation of shocks (Herbold et al. 1985; Fawzy et al. 1998). The dissipation region is indicated by the shaded cloud (representing a cloud of heated gas) in Fig. 3. This heated cloud radiates at wavelengths typical of the chromosphere. Clearly, since it is relatively optically thin, this cloud radiates in all directions, which

qualitatively explains why, e.g., the contrast of magnetic features in CaII K is equally large at all locations on the solar disc.

The increase in the contrast with magnetic flux or magnetogram signal seen in Fig. 2b at small $H_{||}$ is explained by the increasing density of magnetic flux tubes as the magnetic flux increases (Solanki et al. 1991; Fawzy et al. 1998) and the saturation at large $H_{||}$ by a decreased excitation rate of waves as a large density of flux tubes starts affecting the granules around them (Title et al. 1989). However, unlike in the photosphere, the chromospheric brightness does not decrease with increasing B (outside of sunspots).

So far much of the theoretical work on flux-tube waves suffers from the fact that the computations are restricted to 1-D models. Recent 2-D simulations, as described by Carlsson and Hansteen (2005), as well as planned 3-D simulations, show considerable promise for significant progress in this field.

Sunspots are dark in the photosphere and the lower chromosphere, while in the upper chromosphere and the transition region they are either neutral (i.e. at a similar brightness as the quiet Sun), or are bright (in particular the penumbrae). This suggests that although in the photosphere the large surface area of the sunspots relative to their circumference is the dominent reason for sunspot darkness (the quenching of the convective energy transport can be only partly compensated by the inflow of radiation through the side walls), in the chromosphere the magnetic heating mechanisms appear to work for them as well, although not with the same efficiency as in the magnetic elements.

Using the above information we can now attempt to explain the qualitative solar cycle behaviour shown by the irradiance from different atmospheric layers in Fig. 1. Basically, the difference is due to the fact that the photospheric radiation gets enhanced contributions from the magnetic elements, and depressed contributions from the sunspots. The fact that the sunspot contrast is much larger than the contrast of magnetic elements leads to the strong downward deflection of the TSI. In the chromosphere the influence of the magnetic elements is enhanced (stronger contrast in the chromosphere) and the influence of the sunspots is small (even neutral), leading to a larger variation of the chromospheric irradiance, with most of the variations being due to the plage regions. Finally, the corona shows a similar behaviour as the chromosphere, but with some differences due to the fact that coronal loops, whose heating mechanism is different again, contribute to a large extent, which explains the even lower correlation with the TSI.

The increased correlation between TSI and the other indicators for the running monthly means is due to the fact that the darkening due to a particular spot or a group of sunspots usually lasts a week or less, whereas the plages within active regions firstly display a brightening for the full two weeks that they remain visible per solar rotation (the enhanced contrast near the limb roughly compensates for the smaller projected area, etc.), and, secondly, they live for a much longer time. Consequently, the same patches of plage will in general be visible over multiple cycles. Finally, plage is distributed much more homogeneously over the solar surface than sunspots. All these effects work to smooth out the short-term irradiance variations due to plage compared to those due to sunspots. At longer time scales, therefore, both photospheric and chromospheric irradiance are dominated by the influence of plages.

5. Quantitative Reconstruction of Irradiance: SATIRE Models

Models aiming to quantitatively reproduce solar irradiance variations can be divided into two classes. The first class contains those models that use the correlation between the irradiance to be modelled and one or more activity indicators as the basis for the reconstruction. The second class of models employs model atmospheres of different types of magnetic features to compute their spectra. These spectra are then combined according to the area covered by each type of feature to get the irradiance.

The Spectral And Total Irradiance REconstrution (SATIRE) model (Fligge et al. 2000; Krivova et al. 2003) is a successful example of the second type of model. The results obtained by other models that use model atmospheres to compute the spectral irradiance have been published by Fontenla et al. (2004); Haberreiter et al. (2005); Fontenla and Harder (2005) and Harder et al. (2005).

These models have in common that they divide the solar surface into features (components), which are assumed to have universal properties (e.g., all sunspot umbrae and penumbrae are assumed to be well-described by the same time-independent model atmosphere). The number of such atmospheric components differs from model to model. In the case of the SATIRE models, 4 atmosphere components are deemed sufficient: sunspot umbrae, sunspot penumbra, quiet Sun and faculae (the network elements are described by the same atmospheric parameters, although this is known not to be strictly correct; e.g., Solanki & Stenflo 1984; Solanki 1986). The evolution of these components is deduced from the observed evolution of the magnetic field at the solar surface (from magnetograms in the case of SATIRE, from brightness images in the case of other models). More details can be found in Fligge et al. (2000), Krivova et al. (2003), Krivova & Solanki (2005), Wenzler et al. (2006).

The SATIRE model has successfully reconstructed the TSI over 3 decades. E.g., it is found that over 90% of the TSI variations in cycle 23, for which the best data are available, are due to the magnetic field at the solar surface.

In spite of this success there are a few important shortcomings of the SATIRE models. Firstly, there is a free parameter that can be adjusted in order to obtain a good match to the TSI data. Secondly, and more importantly for chromospheric irradiance variability, the spectra computed in the context of SATIRE are in LTE, since it is mainly aimed at reproducing the photospheric signature of irradiance variations.

An overview of the important NLTE-based work in this field is given by Fontenla (2007). Whereas in LTE all strong lines display a large amplitude of the solar cycle variation, the measurements show that the lines actually behave rather differently. Two extreme examples are the Mg I 285.21 nm and the Mg II h and k resonance lines. Whereas the emission core of the latter varies strongly over the cycle (to the extent that the Mg II core-to-wing ratio is used as a standard indicator for solar activity; see Fig. 1), the core of the Mg I resonance line shows very little variation. This behaviour has been explained and reproduced by the non-LTE computations of Uitenbroek and Briand (1995). SATIRE reproduces the Mg II variability, but not that of the Mg I resonance line due to the restriction of the model to LTE (Unruh et al. in preparation).

This implies the need for an empirical extension of SATIRE in order to reproduce the variability at shorter wavelengths. This can be achieved by mak-

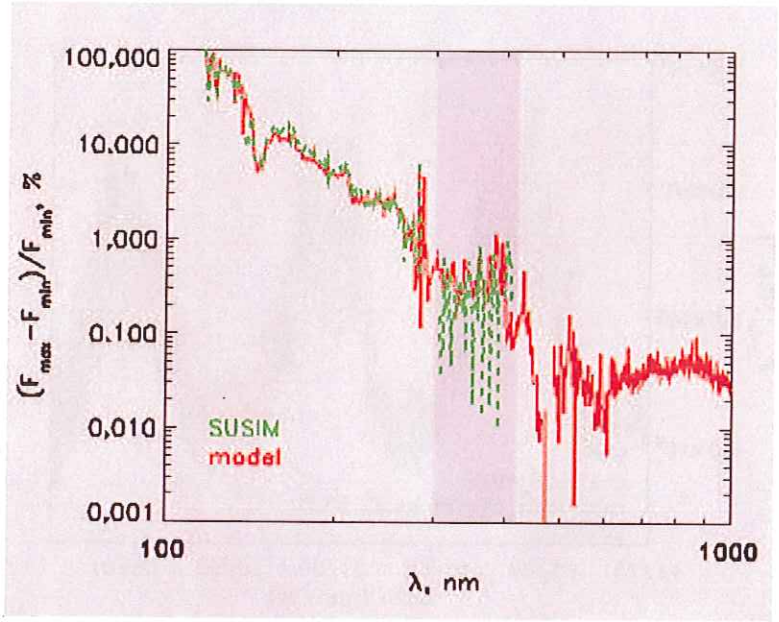

Figure 4. Relative difference between the spectral irradiance at solar activity maximum (averaged over a two month period, April-May 2000) and at solar activity minimum (October-November 1996). Plotted are the results obtained by the SUSIM instrument (dashed curve; green in the electronic version) and computed by the SATIRE model, including its empirical extension to shorter wavelengths (solid curve; red in the electronic version). Figure adapted from Krivova et al. (2006).

ing use of the good correlation between SATIRE and, e.g., SUSIM (Vanhoosier et al. 1981) data at individual wavelengths (e.g., Mg II core or the continuum around 220-240 nm), as well as the good correlation between the irradiance at different SUSIM wavelengths. Together these relationships allow us to use magnetograms to reconstruct the spectral irradiance variations down to Ly-α wavelengths (Krivova et al. 2006). In Fig. 4 we show the relative difference between the maximum and minimum of solar cycle 23 as measured by SUSIM and as computed by SATIRE (including its empirical extension to shorter wavelengths). Note the logarithmic wavelength scale. The uncertainties in the SUSIM data are larger than the relative variability at $\lambda > 300$ nm and it generally underestimates the variability there. Clearly, for the wavelengths at which SUSIM does give reliable data, both model and reconstruction agree relatively well with each other. We stress that these reconstructions were carried out with the same value of the SATIRE free parameter as used for the TSI reconstructions.

Of particular interest for the upper atmosphere of the Earth is the irradiance variability of the Ly-α line, since its radiation is absorbed by NO_x in layers above the stratosphere. Consequently, considerable work has been done to reconstruct the variations in this line. These have culminated in the composite of Ly-α variations (Woods et al. 2000) based on measurements from SOLSTICE (SOLar Stellar Irradiance Climate Experiment; Rottman et al. 1993) on the

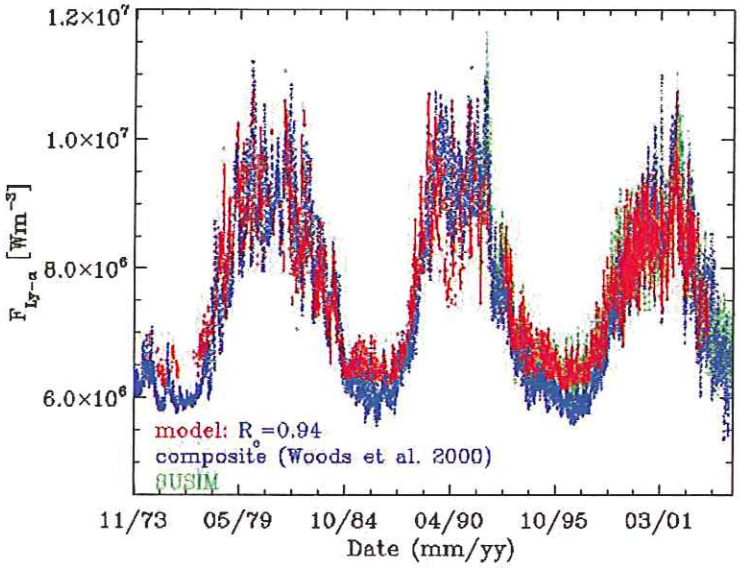

Figure 5. Composite of Ly-α irradiance (blue curve in electronic version) based on UARS/SOLSTICE and other satellite measurements, as well as proxy models, compared with the reconstruction of Ly-α irradiance reconstructed using the empirically extended SATIRE model (red curve) and the UARS/SUSIM measurements (green curve). The correlation coefficient between the synthetic SATIRE-based Ly-α irradiance and the composite is indicted. Figure kindly provided by N. A. Krivova.

UARS spacecraft, other instruments and proxy models (used to fill in the gaps and extend the time series further back in time). In Fig. 5 this composite is plotted (in blue in the electronic version). Also plotted (in green) are the SUSIM data and (in red) the SATIRE reconstruction. Once again, the same value of the free parameter was used as for the TSI reconstructions. It is noticeable that although the general agreement between the model and the composite is very good, the amplitude of the solar cycle variation is underestimated by roughly 5% by the SATIRE model. However, the agreement with the SUSIM data, which was originally used to calibrate and extend the model to shorter wavelengths is far better.

This success of modeling the variability of chromospheric irradiance bodes well for long-term reconstructions of this quantity. By combining the extended SATIRE reconstruction method with computations of the evolution of the magnetic field, it should be possible to deduce the Ly-α irradiance back to 1611, the start of telescopic observations of the Sun.

6. Evidence for Pumping between Mg II and Mn I?

W. Livingston has been regularly measuring disk integrated spectra of a series of visible lines for 3 decades (e.g., Livingston et al. 2006). A number of these

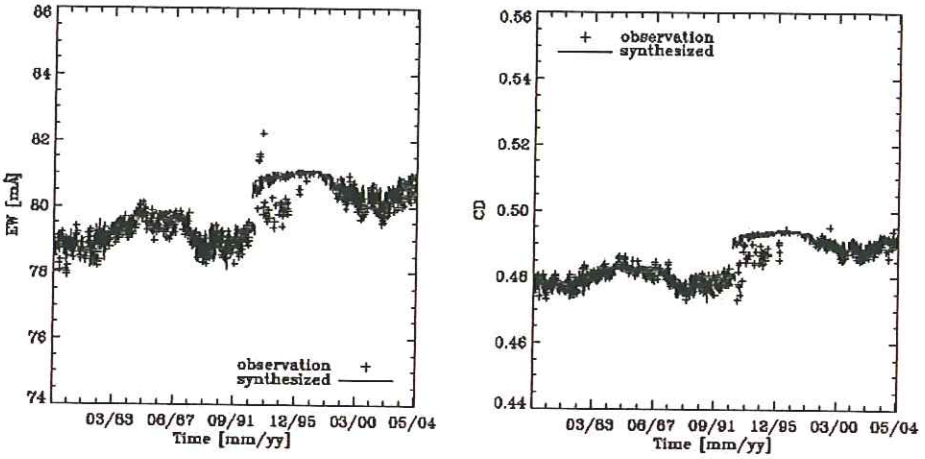

Figure 6. Equivalent width (*EW*, left panel) and line depth (*LD*, right panel) of the Mn I 5394 Å line vs. time. The crosses refer to values measured by W. Livingston, the solid curve to the synthesized *EW* and *LD* obtained from the SATIRE model. Figure adapted from Danilovic et al. (2007).

lines display a cyclic behaviour in their equivalent widths (*EW*), with the most prominent such behaviour being shown by the Ca II K line core. In general the photospheric lines display a strongly reduced cyclic variation. Some lines, such as Fe I 5395 Å hardly shows any variation at all. In contrast, the Mn I 5394 Å line, which is formed in the photosphere, displays a very clear cyclic signature. Its *EW* decreases during periods of high activity, i.e., it varies in antiphase with the sunspot number or Mg II k core-to-wing ratio. The measured Mn I *EW* and line depth are plotted vs. time in Fig. 6. They are represented by the crosses. Changes were made to the spectrograph in 1992, which led to an offset in the measured *EW* and line depth. Trials with the new instrument lasted until 1996, so that only the data prior to 1992 and after 1996 should be considered for any subsequent analysis (Livingston, private communication).

The uncharacteristically large variability of the Mn I lines at 5394 and 5432 Å led Doyle et al. (2001) to propose that these Mn I lines are very sensitive to optical pumping by the Mg II k line. An alternative explanation may be due to a particularly large temperature sensitivity of these lines. This was first pointed out by Elste (1985, 1987).

Using SATIRE it is possible to distinguish between these two alternative scenarios by carrying out computations of the Mn I 5394 Å line assuming LTE, but taking into account the influence of the evolving surface magnetic field. In Fig. 6 the synthetic Mn I *EW* and line depth values are represented by the solid lines. The effects of the change in instrumental parameters are taken into account in a simple way. This introduces a free parameter, which basically influences the magnitude of the offsets in these two quantities between 1992 and 1996, but does not significantly influence the amplitude of the solar cycle variation seen in the parameters of this line. Note that the free parameter of the

SATIRE model is, once more, fixed to the value given by the TSI reconstruction. The fact that the variation of the parameters of the synthetic Mn I line agrees relatively well with the measured values, although the former were computed entirely in LTE suggests that optical pumping does not play a dominant role in explaining the behaviour of this line. More details on this work can be found in Danilovic et al. (2007).

An alternative approach to tackling this question has been taken by Vitas et al. (2007). They explicitly include the pumping and compare its influence compared to other processes.

7. Does the Quiet Sun Change over the Solar Cycle at Chromospheric Layers?

An intriguing question, in particular for the understanding of the secular variation of solar irradiance, is whether the quiet Sun changes over the solar cycle. For the photosphere, after some false alarms (e.g., Kuhn et al. 1988) which have recently been defused (Woodard & Libbrecht 2003), there is no definite evidence of a strong cyclic variation of the quiet Sun. This may, however, be different in the chromosphere, where a much smaller fraction of the total solar irradiance is emitted, so that it is energetically not so challenging to produce a variation of the quiet Sun emission from these layers.

Intriguingly, Schühle et al. (2000) found that the radiance of a quiet Sun region near disk center does increase significantly from solar activity minimum towards maximum in UV lines measured by the SUMER instrument. The analysed lines are formed in the chromosphere, transition region and corona. There is also some, although somewhat less strong, evidence for a change in quiet Sun millimeter wavelength radiation (Loukitcheva 2005), which implies a change in chromospheric thermal structure.

Pauluhn and Solanki (2003) showed that the amount of magnetic flux in the quiet Sun regions studied by Schühle et al. (2000) evolves significantly with time with a good correlation between the radiance and the amount of magnetic flux. Figure 7 illustrates the correspondence between the magnetic flux and the radiance of the He I 504 Å line averaged over the considered quiet Sun regions. It seems that absolutely quiet Sun can hardly be found near the equator of the Sun at the time around activity maximum. The decaying active regions keep feeding the seemingly quiet Sun with additional magnetic flux faster than it can be transportrd away. This build up of magnetic flux in the quiet Sun is the main reason for any observed changes in radiation coming from there. Note that the large patches of unipolar field resulting from the decay of active regions decay far more slowly than the mixed polarity network maintained by the emergence of ephemeral active regions (Harvey 1993; Hagenaar et al. 2003).

In summary, changes in chromospheric radiance of the quiet Sun over cycle 23 are coupled with the evolution of the magnetic field and thus with the evolution of photospheric radiance.

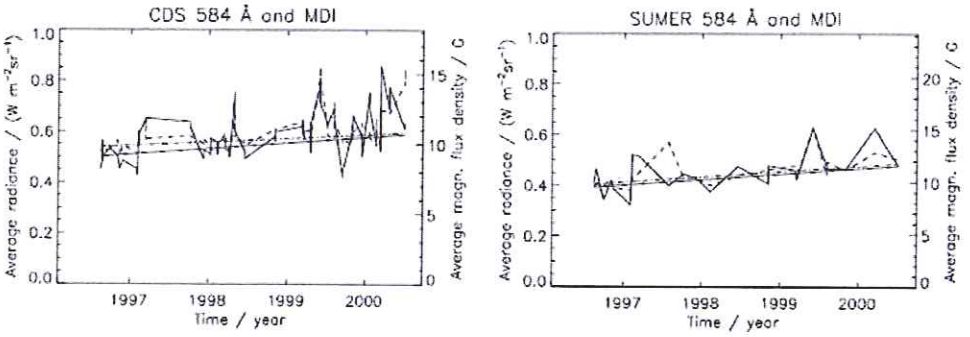

Figure 7. Time series of the spatially averaged radiances of the He I 584 Å line and corresponding MDI/SOHO magnetic fluxes. The radiances were obtained by the CDS and SUMER spectrometers on SOHO. The solid lines represent the radiance data and their linear fits, the dashed and dot-dashed lines refer to the MDI data and their corresponding fits. The plotted fits indicate an increase between 15% (MDI in CDS sampling) and 22% (SUMER) within the four years from June 1996 to June 2000. Figure taken from Pauluhn and Solanki (2003).

8. Steps towards Determining Secular Variations of Solar Chromospheric Irradiance

The question of whether there is a secular variation of chromospheric irradiance is closely related to the similar one whether total solar irradiance also shows a secular change. This is because significant secular change in the irradiance can only be due to a change in the quiet Sun contribution to it (since the active region contribution all but disappears at the time of activity minimum) and variations of the chromospheric radiance of the quiet Sun are related to photospheric variations, as argued in the previous section. Similarly, we expect secular changes in the chromospheric radiation to depend on such changes in the magnetic field, although we cannot rule out other causes as well (e.g., variations in the "basal flux" of chromospheric radiation; e.g., Schrijver et al. 1989).

Only measurements that are available over a long period of time can be used for estimating secular change of the Sun's irradiance (including the chromospheric contribution). The direct solar measurements that have so far mainly been used to consider this question are measurements of sunspot number and area. These are, on their own, insufficient to give a proper answer to this question. Indirect evidence is provided by the reconstruction of the interplanetary magnetic field (which is a good proxy of the Sun's open magnetic flux according to measurements by the Ulysses spacecraft) by Lockwood et al. (1999). The reconstruction shows that the open flux has doubled over the last century. Does this doubling imply also an increase of total magnetic flux and consequently irradiance?

The basic idea to explain this doubling of open flux makes use of the concept of overlapping solar activity cycles, which follows from the extended solar cycle postulated by Wilson et al. (1988). Such an overlap can be produced by the long lifetime (decay time) of magnetic flux. In general, it is magnetic flux having the same polarity on large spatial scales, which usually corresponds to open magnetic

flux, which has a long lifetime (Solanki et al. 2000; Solanki & Schüssler 2005). A second process that can lead to an overlap between cycles is if magnetic flux belonging to the new cycle starts appearing while there is still active region flux belonging to the old cycle present at the solar surface. Ephemeral active regions have been shown to have an emergence cycle which lasts longer and may be shifted in phase relative to the cycle of the normal active regions (Harvey 1992; 1993; Hagenaar et al. 2003). In this case, since ephemeral regions contribute very significantly to the total amount of flux emerging at the solar surface, the total magnetic flux could also show a secular change (Solanki et al. 2002; Baumann et al. 2004; Solanki & Schüssler 2005).

However, there is still considerable uncertainty regarding the magnitude of the secular variation of the total magnetic flux. Different recent estimates lie widely apart from each other.

Historical records of images made in the cores of strong chromospheric lines have the potential to help resolve some of these open questions. In particular, spectroheliograms in the cores of the CaII K line, as have been recorded over many decades at different observatories including Kodaikanal, Mt. Wilson, Arcetri and, last but not least, Coimbra. For a more complete list see Ermolli et al. (2007).

The spectroheliograms were recorded on film which has an *a priori* unknown non-linear blackening curve and they also suffer from other artifacts. Unfortunately, these images have either no calibration information associated with them, or this information is inadequate (in particular for the older and hence more valuable images).

There are two approaches to utilizing these data: Foukal (1996) and Foukal & Milano (2001) have neglected all problems and have simply taken the images at face value. Although this approach is straightforward and simple, it is at best limited to drawing qualitative conclusions.

I. Ermolli, A. Tlatov and others have, in contrast, put great care into determining the calibration as best as possible and into removing as many of the artifacts as possible prior to carrying out any analysis of these data. The latter approach, which, in a first step, is being applied to Kodaikanal, Arcetri and Mt Wilson data, promises superior results, but is still in the process of being developed. It is clear that the Coimbra archive will play an important role in this effort, once these data are digitized. Only a careful intercomparison between images obtained at different locations can uncover all the artifacts and validate the results obtained from CaII K spectroheliograms (e.g., by catching often undocumented changes in the instrumentation, or picking out images degraded strongly by poor seeing). See the paper by Ermolli et al. (2007) for more details. Furthermore, the so far considered data sets contain many gaps, so that the availability of a further data set is very valuable to fill these. The Coimbra dataset will thus play an important role in answering the question of the magnitude of the secular change of solar total and spectral irradiance. It will in particular also help to determine the chromospheric contribution to such change.

9. Conclusion

The cyclic and secular variation of chromospheric radiation is of considerable importance for a variety of questions related to the physics of magnetic elements, to the evolution of solar magnetism and activity, and to the variation of total and spectral solar irradiance. Radiation from the chromosphere, due to its large variability (compared to the photospheric radiation) and due to the ease of measurement (compared to transition region and coronal emission), often serves as a useful proxy of solar activity, magnetism or total solar irradiance. In many ways chromospheric radiation is superior to the generally used sunspot number or area records employed to reconstruct activity and irradiance further back in time. The availability of historical records of chromospheric radiation (basically spectroheliograms of CaII K core intensity) reaching back to the early part of the 20th century is exciting and holds the promise to answer the fundamental question regarding the secular variation of solar activity and irradiance: how strong were these changes? The data set recorded in Coimbra will surely play an important role in such an effort.

Acknowledgments. Many people helped to make this paper become a reality. My thanks go to the organizers for their kindness and to the editors for their patience, to N. Krivova and S. Danilovic for providing figures prior to publication, and to B. Wieser, P. Daly and B. Podlipnik for technical help.

References

Baumann, I., Schmitt, D., Schüssler, M., & Solanki, S. K. 2004, A&A, 426, 1075
Carlsson, M., & Hansteen, V. 2005, in Chromospheric and Coronal Magnetic Fields, Eds. Innes, D. E., Lagg, A. & Solanki, S. K., ESA SP-596
Danilovic S., Solanki S.K., Krivova N.A., & Livingston W. 2007, in Modern Solar Facilities – Advanced Solar Science, Eds. F. Kneer et al., Universitätsverlag Göttingen, in press
Deinzer, W., Hensler, G., Schuessler, M., & Weisshaar, E. 1984a, A&A, 139, 426
Deinzer, W., Hensler, G., Schussler, M., & Weisshaar, E. 1984b, A&A, 139, 435
Deland, M. T., & Cebula, R. P. 1998, Solar Phys., 177, 105
Dewitte, S., Crommelynck, D., Mekaoui, S., & Joukoff, A. 2004, Solar Phys., 224, 209
Doyle, J. G., Jevremović, D., Short, C. I., Hauschildt, P. H., Livingston, W., & Vince, I. 2001, A&A, 369, L13
Elste, G. 1985, in Theoretical Problems in High Resolution Solar Physics, Ed. H.U. Schmidt, Max Planck Inst. f. Astrophys., 185
Elste, G. 1987, Solar Phys., 107, 47
Ermolli et al. 2007, in P. Heinzel, I. Dorotovič, R. J. Rutten (eds.), The Physics of Chromospheric Plasmas, ASP Conf. Ser. 368, 533
Fawzy, D. E., Ulmschneider, P., & Cuntz, M. 1998, A&A, 336, 1029
Fligge, M., Solanki, S. K., & Unruh, Y. C. 2000, A&A, 353, 380
Fontenla, J. 2007, in P. Heinzel, I. Dorotovič, R. J. Rutten (eds.), The Physics of Chromospheric Plasmas, ASP Conf. Ser. 368, 499
Fontenla, J., & Harder, G. 2005, Mem. Soc. Astron. It., 76, 826
Fontenla, J. M., Harder, J., Rottman, G., Woods, T. N., Lawrence, G. M., & Davis, S. 2004, ApJ Lett., 605, L85
Foukal, P. 1996, Geophys. Res. Lett., 23, 2169
Foukal, P., & Milano, L. 2001, Geophys. Res. Lett., 28, 883
Frazier, E. N. 1971, Solar Phys., 21, 42

Fröhlich, C. 2005, Mem. Soc. Astron. It., 76, 731
Haberreiter, M., Krivova, N. A., Schmutz, W., & Wenzler, T. 2005, Adv. Space Res., 35, 365
Hagenaar, H. J., Schrijver, C. J., & Title, A. M. 2003, ApJ, 584, 1107
Harder, J., Fontenla, J., White, O., Rottman, G., & Woods, T. 2005, Mem. Soc. Astron. It., 76, 735
Harvey, K. L. 1992, The Solar Cycle, in ASP Conf. Ser., Vol. 27, 335
Harvey, K. L. 1993, Ph.D. Thesis, Magnetic Dipoles on the Sun, University of Utrecht, Utrecht
Heath, D. F., & Schlesinger, B. M. 1986, J. Geophys. Res., 91, 8672
Herbold, G., Ulmschneider, P., Spruit, H. C., & Rosner, R. 1985, A&A, 145, 157
Huang, P., Musielak, Z. E., & Ulmschneider, P. 1995, A&A, 297, 579
Krivova, N. A., & Solanki, S. K. 2005, Mem. Soc. Astron. It., 76, 834
Krivova, N. A., Solanki, S. K., Fligge, M., & Unruh, Y. C. 2003, A&A, 399, L1
Krivova, N. A., Solanki, S. K., & Floyd, L. 2006, A&A, 452, 631
Kuhn, J. R., Libbrecht, K. G., & Dicke, R. H. 1988, Science, 242, 908
Livingston, W., Wallace, L., White, O. R., & Giampapa, M. S. 2006, ApJ, in press
Lockwood, M., Stamper, R., & Wild, M. N. 1999, Nature, 399, 437
Loukitcheva, M. 2005, The structure and dynamics of the solar chromosphere from observations at millimeter wavelengths, Ph.D. thesis, Saint-Petersburg University, Russia.
Mathew S., Martínez Pillet V., Solanki S.K., & Krivova N.A. 2007, A&A, in press
Mitchell, W. E., Jr., & Livingston, W. C. 1991, ApJ, 372, 336
Musielak, Z. E., & Ulmschneider, P. 2002, A&A, 386, 606
Musielak, Z. E., Rosner, R., & Ulmschneider, P. 2000, ApJ, 541, 410
Narain, U., & Ulmschneider, P. 1996, Space Sci. Rev., 75, 453
Noble, M. W., Musielak, Z. E., & Ulmschneider, P. 2003, A&A, 409, 1085
Ortiz, A., Solanki, S. K., Domingo, V., Fligge, M., & Sanahuja, B. 2002, A&A, 388, 1036
Pauluhn, A., & Solanki, S. K. 2003, A&A, 407, 359
Roberts, B. & Ulmschneider, P. 1997, European Meeting on Solar Physics, Eds. Simnett, G. M., Alissandrakis, C. E. & Vlahos, L., Lecture Notes in Physics, Vol. 489, 75
Roberts, B. & Webb, A. R. 1978, Solar Phys., 56, 5
Rottman, G. J., Woods, T. N., & Sparn, T. P. 1993, J. Geophys. Res., 98, 10667
Schrijver, C. J., Cote, J., Zwaan, C., & Saar, S. H. 1989, ApJ, 337, 964
Schühle, U., Wilhelm, K., Hollandt, J., Lemaire, P., & Pauluhn, A. 2000, A&A, 354, L71
Solanki, S. K. 1986, A&A, 168, 311
Solanki, S. K., & Stenflo, J. O. 1984, A&A, 140, 185
Solanki, S. K., & Schüssler, M. 2005, Mem. Soc. Astron. It., 76, 781
Solanki, S. K. & Unruh, Y. C. 1998, A&A, 329, 747
Solanki, S. K., Steiner, O., & Uitenbroeck, H. 1991, A&A, 250, 220
Solanki, S. K., Schüssler, & M., Fligge, M. 2000, Nature, 408, 445
Solanki, S. K., Schüssler, M., & Fligge, M. 2002, A&A, 383, 706
Steiner, O., Grossmann-Doerth, U., Schussler, M., & Knolker, M. 1996, Solar Phys., 164, 223
Tapping, K. F. 1987, J. Geophys. Res., 92, 829
Tapping, K. F., & Detracey, B. 1990, Solar Phys., 127, 321
Title, A. M., Tarbell, T. D., Topka, K. P., Ferguson, S. H., Shine, R. A., & SOUP Team 1989, ApJ, 336, 475
Topka, K. P., Tarbell, T. D., & Title, A. M. 1997, ApJ, 484, 479
Uitenbroek, H., & & Briand, C. 1995, ApJ, 447, 453
Unruh, Y. C., Solanki, S. K., & Fligge, M. 1999, A&A, 345, 635
Vanhoosier, M. E., Bartoe, J.-D. F., Brueckner, G. E., Prinz, D. K., & Cook, J. W. 1981, Solar Phys., 74, 521

Viereck, R. A., & Puga, L. C. 1999, J. Geophys. Res., 104, 9995
Viereck, R., Puga, L., McMullin, D., Judge, D., Weber, M., & Tobiska, W. K. 2001, Geophys. Res. Lett., 28, 1343
Vitas, N., Vince, I., Danilović, S., & Andriyenko, O. 2007, in P. Heinzel, I. Dorotovič, R. J. Rutten (eds.), The Physics of Chromospheric Plasmas, ASP Conf. Ser. 368, 543
Vögler, A., Shelyag, S., Schüssler, M., Cattaneo, F., Emonet, T., & Linde, T. 2005, A&A, 429, 335
Wenzler, T., Solanki, S. K., Krivova, N. A., & Fröhlich, C. 2006, A&A, 460, 583
Wilson, P. R., Altrock, R. C., Harvey, K. L., Martin, S. F., & Snodgrass, H. B. 1988, Nature, 333, 748
Willson, R. C., & Mordvinov, A. V. 2003, Geophys. Res. Lett., 30, 3
Woodard, M. F., & Libbrecht, K. G. 2003, Solar Phys., 212, 51
Woods, T. N., Tobiska, W. K., Rottman, G. J., & Worden, J. R. 2000, J. Geophys. Res., 105, 27195
Zwaan, C. 1978, Solar Phys., 60, 213